Electronic Supplementary Material (ESI) for Dalton Transactions.

Supporting Information
Multi-function Broad-Band Emission $Ba_{4-x-y}Sr_yLa_6O(SiO_4)_6:xEu^{2+}$ Phosphor for White LED, and Anti-counterfeiting

Zhi Wang[1], Xu Li[1,2], Mingyang Li[1], Jinxing Zhao[1], Zhenyang Liu[1], Dawei Wang[3], Li Guan[4*], Fenghe Wang[1,2*]*

[1] Hebei Key Laboratory of Optic-Electronic Information and Materials, College of Physics Science and Technology, Hebei University, Baoding 071002, PR China

[2] National-Local Joint Engineering Laboratory of New Energy Photoelectric Devices, Institute of Life Science and Green Development, Hebei University, Baoding, 071002, PR China

[3] Hebei Key Laboratory of Semiconductor Lighting and Display Critical Materials, Hebei Ledphor optoelectronics technology Co., LTD. Baoding, 071000, PR China

[4] Key Laboratory of High-precision Computation and Application of Quantum Field Theory of Hebei Province, Hebei University, Baoding 071002, PR China

[*] Corresponding author: lguan@hbu.edu.cn (L. Guan); fenghe_wang@hotmail.com (F. H. Wang); lixcn@sina.com (X. Li)

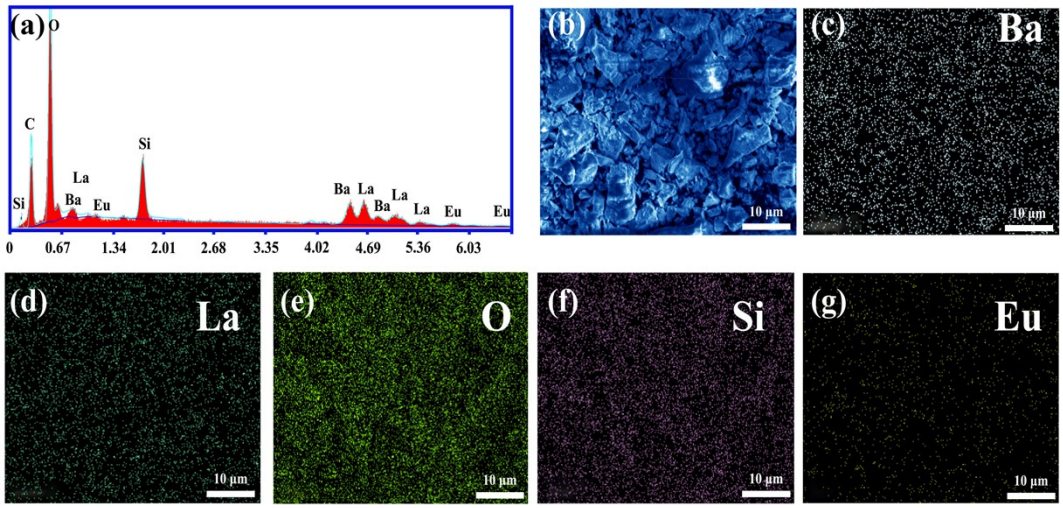

Fig.S1 (a) EDS images and (b) SEM image of BLOS:0.28Eu2+; (c-g) Elemental mapping images of Ba, La, O, Si, and Eu for the selected particle, respectively.

Table S1. Main Crystallographic Parameters for $Ba_{4-x}La_6O(SiO_4)_6$:xEu^{2+} (x = 0.016 − 0.48) from the GSAS Program Rietveld Refinement

concentr	x=0.016	x=0.04	x=0.08	x=0.28	x=0.48
crystal	hexagon	hexagon	hexagon	hexagon	hexagon
space	$P\,6_3/m$	$P\,6_3/m$	$P\,6_3/m$	$P\,6_3/m$	$P\,6_3/m$
***a* = *b* (Å)**	9.807	9.8063	9.8051	9.7904	9.7795
(Å)	7.3454	7.3405	7.3388	7.3231	7.308
***V* (Å^3)**	611.82	611.316	611.021	607.893	605.285
2*θ*	10 - 75°	10 - 75°	10 - 75°	10 - 75°	10 - 75°
R_{wp} (%)	10.92	9.61	11.62	10.62	11.97
R_p (%)	6.95	6.49	7.15	6.75	7.52
***CHI*^{2}**	4.476	3.489	5.086	4.342	6.156

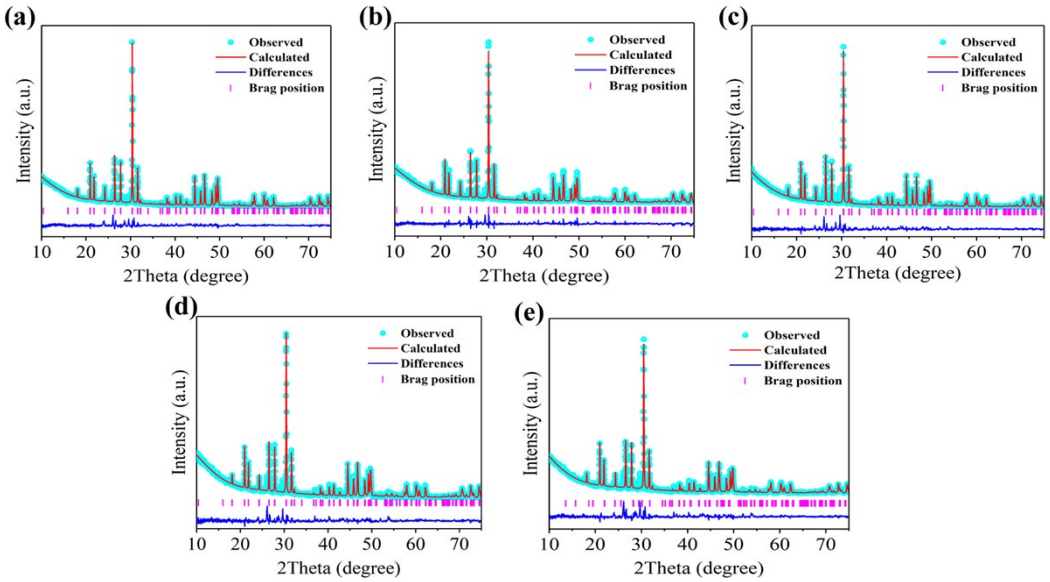

Fig.S2 (a−e) Rietveld refinement of the powder XRD profiles of BLOS:*x*Eu (*x* = 0.016, 0.04, 0.08, 0.28, 0.48), respectively.

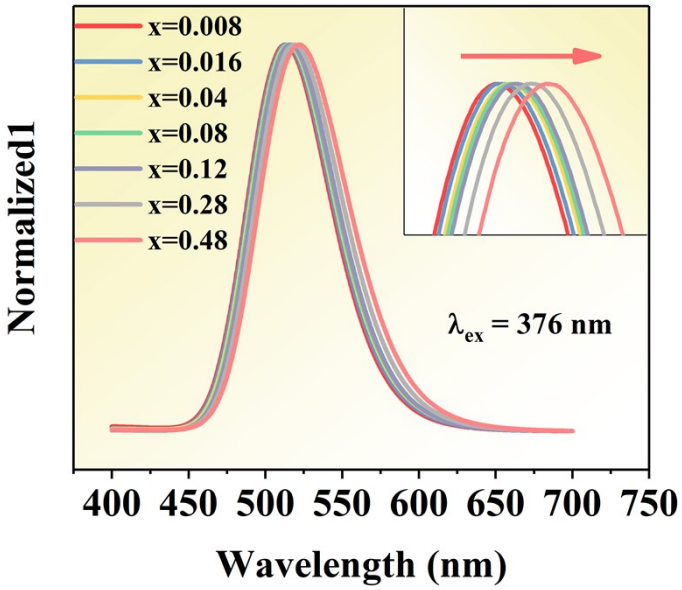

Fig.S3 Normalized PL spectrum of series phosphors BLOS:*x*Eu.

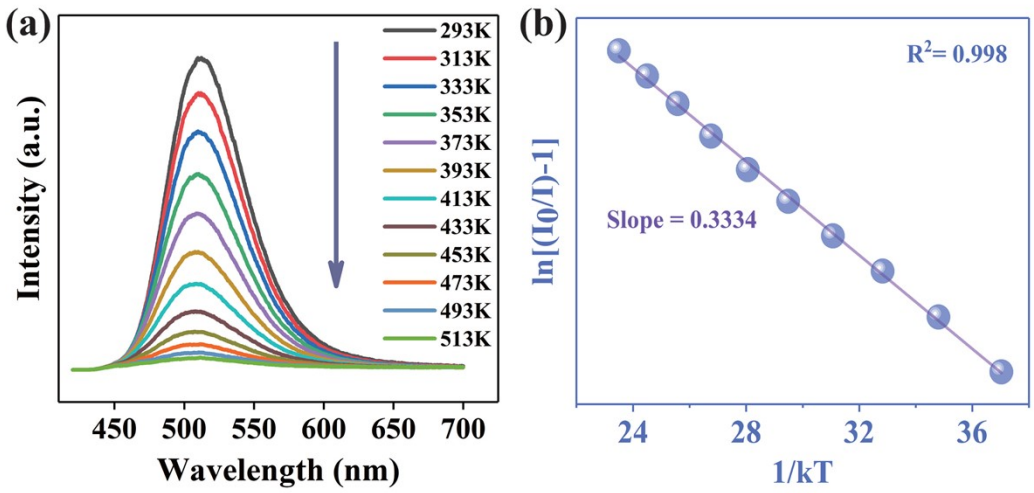

Fig.S4 (a) The temperature-dependent PL spectra of BLOS:0.08Eu phosphors at temperatures of 293−453 K(λ_{ex} = 376 nm); (b) The plot of ln[I_0 /I - 1] versus 1/kT for BLOS:0.08Eu.

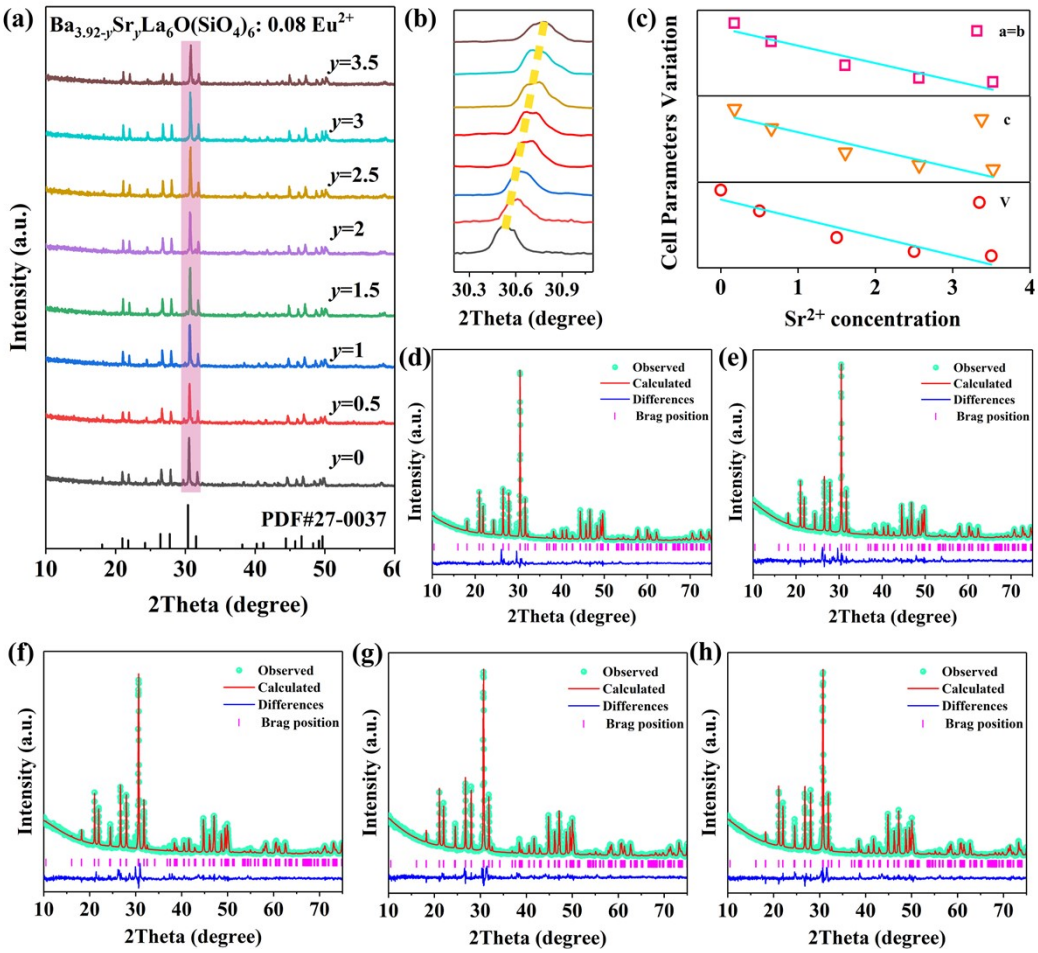

Fig.S5 (a) XRD patterns compared to the standard pattern of $Ba_{3.92-y}Sr_yLa_6O(SiO_4)_6$:0.08Eu ($y$ = 0-3.5) and (b) view of the peak shift at 30.1−31°; (c) evolution of lattice parameters(*a, b, c*) and the unit cell volumes (*V*) for $Ba_{3.92-y}Sr_yLa_6O(SiO_4)_6$:0.08Eu ($y$ = 0, 0.5, 1.5, 2.5, 3.5); (d−h) Rietveld refinement of the powder XRD profiles of $Ba_{3.92-y}Sr_yLa_6O(SiO_4)_6$:0.08Eu.

Table S2. Main Crystallographic Parameters for $Ba_{3.92-y}Sr_yLa_6O(SiO_4)_6$:0.08$Eu^{2+}$ (y = 0 − 3.5) from the GSAS Program Rietveld Refinement

concentration	y=0	y=0.5	y=1.5	y=2.5	y=3.5
crystal system	hexagonal	hexagonal	hexagonal	hexagonal	hexagonal
space group	$P\,6_3/m$	$P\,6_3/m$	$P\,6_3/m$	$P\,6_3/m$	$P\,6_3/m$
***a* =*b* (Å)**	9.8035	9.78	9.7493	9.7329	9.728
***c* (Å)**	7.3405	7.3112	7.2743	7.2553	7.249
***V* (Å^3)**	610.971	605.615	598.777	595.209	594.088
2θ interval	10 - 75°	10 - 75°	10 - 75°	10 - 75°	10 - 75°
R_{wp} (%)	10.69	10.08	10.14	8.54	7.95
R_p (%)	6.66	6.57	6.61	5.78	5.46
CHI^2	5.319	4.898	5.08	3.644	3.604

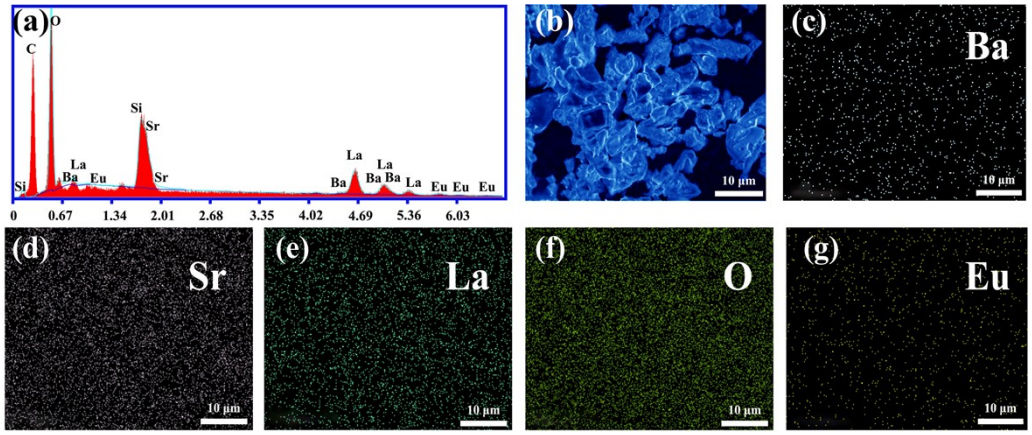

Fig.S6 (a) EDS images and (b) SEM image of $Ba_{1.42}Sr_{2.5}La_6O(SiO_4)_6$:0.08Eu; (c-g) Elemental mapping images of Ba, Sr, La, O and Eu for the selected particle, respectively.

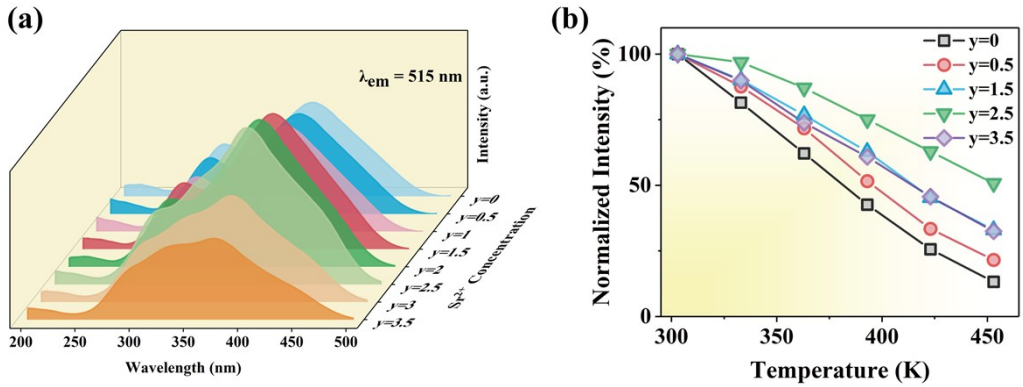

Fig.S7 (a) PL spectra of $Ba_{3.92-y}Sr_yLa_6O(SiO_4)_6$:0.08$Eu^{2+}$ (y = 0−3.5) phosphor; (b) Normalized PL intensity of $Ba_{3.92-y}Sr_yLa_6O(SiO_4)_6$:0.08$Eu^{2+}$ (y = 0−3.5) phosphor at different temperatures.

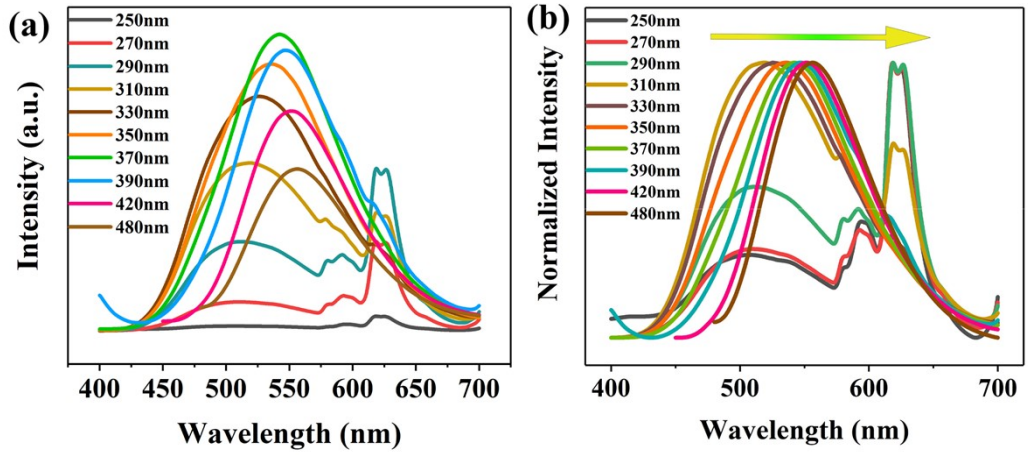

Fig.S8 (a) PL spectra of $Ba_{0.42}Sr_{3.5}La_6O(SiO_4)_6$:0.08$Eu^{2+}$ phosphors at different excitation wavelengths; Normalized PL spectra of $Ba_{0.42}Sr_{3.5}La_6O(SiO_4)_6$:0.08$Eu^{2+}$ phosphors at different excitation wavelengths.

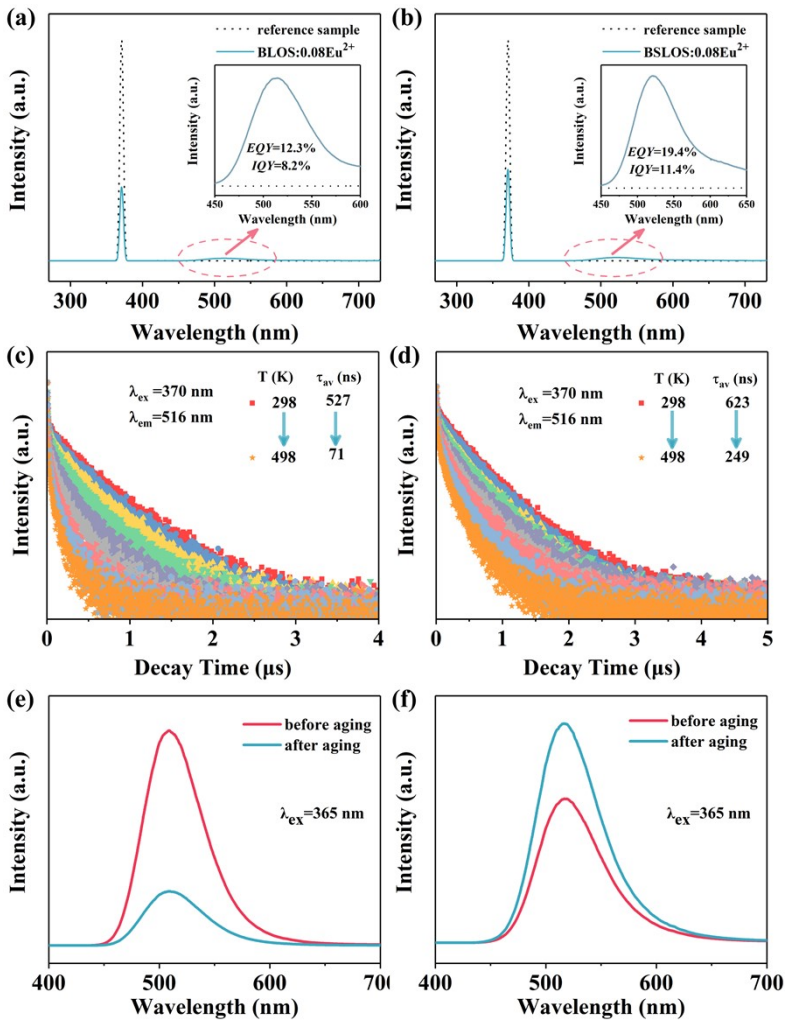

Fig.S9 The quantum efficiency of $Ba_{3.92}La_6O(SiO_4)_6$:0.08Eu phosphors(a) $Ba_{0.42}Sr_{3.5}La_6O(SiO_4)_6$:0.08Eu phosphors(b); The excited-state lifetime dependence on temperature of $Ba_{3.92}La_6O(SiO_4)_6$:0.08Eu phosphors(c) $Ba_{0.42}Sr_{3.5}La_6O(SiO_4)_6$:0.08Eu phosphors(d); The chemical stability of $Ba_{3.92}La_6O(SiO_4)_6$:0.08Eu phosphors(e) $Ba_{0.42}Sr_{3.5}La_6O(SiO_4)_6$:0.08Eu phosphors(f).

Table S3 The chemical stability of $Ba_{3.92}La_6O(SiO_4)_6$:0.08Eu phosphors $Ba_{0.42}Sr_{3.5}La_6O(SiO_4)_6$:0.08Eu phosphors.

	$Ba_{3.92}La_6O(SiO_4)_6$:0.08Eu		**$Ba_{3.92}La_6O(SiO_4)_6$:0.08Eu**	
□	before aging	after aging	before aging	after aging
Normalized intensity	1	0.255	1	0.67
FWHM (nm)	62.14	62.91	66.27	67.3
CIE	(0.19,0.58)	(0.19,0.59)	(0.25,0.61)	(0.24,0.61)
X at max height (nm)	514.2	516.2	524.8	526.2